Synthesis and characterization of neutral Ni(II) and Cu(II) complexes with bidentate $[NS]^{1-}$ ligands

Eric M. Martin and Robert D. Bereman*
North Carolina State University, Department of Chemistry, Box 8204, Raleigh, NC 27695 (U.S.A.)

(Received February 28, 1991; revised June 25, 1991)

Abstract

Bis-bidentate complexes of a series of the type ligands *N*-alkylmethyl-2-aminocyclopentenedithiocarboxylate of Zn(II), Ni(II) and Cu(II) have been prepared and characterized using NMR, ESR, electronic absorption and electrochemical spectroscopy. Methyl, ethyl, n-propyl and n-butyl substituents are found to have subtle effects on the coordination geometry and physiochemical properties of the metal centers. The ligands provide an $[NS]^{1-}$ donor set, which upon chelation, forms a delocalized six member chelate ring with the metal ion in a Schiff base type fashion. Alkyl substituents on the amine nitrogens introduce steric hindrance and drive the coordination stereochemistry from planar to tetrahedral. Spectroscopic data are in support of these geometrical changes, but, interestingly, suggest the maximum distortion of the inner coordination sphere is achieved with the ethyl substituent. Nickel and copper complexes were isolated with the metal in the II oxidation state, except the n-propyl and n-butyl derivatives of copper which were isolated as yellow Cu(I) species. The pseudo-tetrahedral Cu(II) complex where R = ethyl exhibits an intense absorption in the visible region at 16.3 kK and rather low ESR hyperfine splitting of 137×10^{-4} cm^{-1}. The complexes are examined as possible active site models of Ni(II) and Cu(II) N_2S_2 sites in metalloproteins.

Introduction

As part of a continuing effort to design small molecules which can serve as models of metal sites in important biological systems, we have synthesized a series of bis-bidentate zinc, nickel, and copper complexes of the ligands *N'*-alkylmethyl-2-aminocyclopentenedithiocarboxylate which coordinate through two thioketonate sulfurs and two iminato nitrogens (Fig. 1). Interest in coordination compounds with nitrogen and sulfur donor groups stems from the surprising physical properties of metalloenzyme active sites which involve similar coordination, and participate in electron transfer reactions. Consistent among many of the proposed coordination environments for several quite varied metalloenzymes is a distorted four coordinate N_2S_2 donor set.

Perhaps the most studied N_2S_2 system is that of the type I blue copper(II) proteins, which involve Cu(II) ions ligated to two nitrogens from histidine residues, a sulfur from a cysteine residue, and a thioether linkage via a methionine group [1]. ESR studies have shown the coordination environment is tetrahedrally distorted and low in symmetry, giving rise to a rhombic signal with very small metal hyperfine values [2]. The blue copper sites in proteins derive their name from a low energy electronic transition

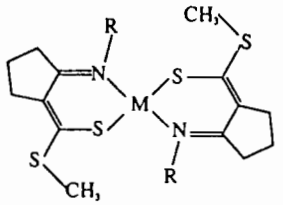

R = me (a), et (b), n-pr (c), and n-bu (d)

M = Ni(II) (1), Cu(II) (2), and Zn(II) (3)

(a)

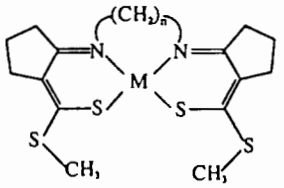

n = 0, 2, 3, 4, and 5

M = Ni(II) (4), Cu(II) (5), and Zn(II) (6)

(b)

Fig. 1. Lewis structures of $M(II)N_2S_2$ model systems.

*Author to whom correspondence should be addressed.

0020-1693/91/$3.50

of unusually high intensity, which is assigned as a σS(cys)–Cu(II) LMCT ($\epsilon = 3000\ cm^{-1}\ M^{-1}$) [3]. The abnormal ESR parameters and low energy S–Cu(II) LMCT are frequently the goals of synthetic approaches designed to produce simple inorganic model systems [4, 5]. Many small molecule systems have been designed and characterized, however, a complete understanding of the protein active site and Cu(II)/Cu(I) redox mechanism is still missing [6].

Since the discovery of the nickel centers in certain hydrogenases, CO dehydrogenases and methyl coenzyme reductases, efforts have also centered around defining the stabilizing effects nitrogen and sulfur donor atoms exert on nickel in various oxidation states [7]. The native enzymes involve a redox couple for Ni(II)/Ni(III) far less positive (−150 to −450 mV) than that normally achieved in synthetic complexes. Experiments using electron spin resonance, X-ray diffraction and X-ray absorption techniques suggest one to four sulfurs bind a monomeric nickel ion at the hydrogenase active site, with the remaining coordination sites filled by either nitrogen or oxygen donors [8]. Common to many proposed active site models are combinations of sulfur, nitrogen and oxygen donors in planar and distorted four coordinate environments. N_2S_2, N_2SO, NS_3 and S_4 systems have been investigated [9–12], and one highly anionic square planar $[N_2S_2]^{4-}$ environment has exhibited marked stabilization of trivalent nickel [9a].

The convenient spectroscopic properties of d^8 Ni(II) also make it a preferred substitute in metal replacement studies, many of which have involved the blue sites in copper proteins [13]. The fast relaxation times and sensitive ligand field transitions make nickel(II) an excellent probe for studies on the magnetic and stereoelectronic properties of complexes.

Earlier work by this group produced the series of related tetradentate N_2S_2 ligands *N,N'*-ethylenebis-, trimethylenebis- and tetramethylenebis(methyl 2-amino-1-cyclopentenedithiocarboxylate), which when chelated to Cu(II) and Ni(II) 'trapped' stereochemistries at various points along the square planar–tetrahedral equilibrium (Fig. 1(b): **4** and **5**, $n = 2$, 3 and 4) [14, 15]. By increasing the number of methylene groups in the bridge between the two nitrogens, three Cu(II) complexes were stabilized with dihedral angles between CuSS' and CuNN' planes that varied from 20° to 54° to 57°, for **5** $n = 2$, 3 and 4, respectively. The analogous Ni(II) series yielded complexes with smaller dihedral angles of 3, 18 and 36°, for **4** $n = 2$, 3 and 4. As expected the Ni(II) complexes remain more square planar. Our present goals are to attempt to stabilize even more distorted Ni(II) and Cu(II) complexes by both extending the methylene bridge between the nitrogens, and by adding progressively bulkier aliphatic residues to the parent methyl-2-aminocyclopentenedithiocarboxylate ligand. Quantitative relationships between structures and trends in physical properties established in the earlier work allow assignment of stereochemistries by analogy. Thus, we have now characterized a new series of four coordinate complexes where changes in physical, geometric and stereoelectronic properties are produced as a function of the alkyl substituent added to the amine nitrogen. In lieu of crystal structure analyses, stereochemistries are proposed on the basis of ESR parameters and NMR spectral data of the respective Cu(II) and Ni(II) complexes. A single crystal and molecular structure analysis of **1b** is currently underway, and will be reported upon full refinement.

Experimental

Materials

All reagents and solvents were commercially obtained from Fisher Scientific and Aldrich Chemicals, and used without further purification. Tetraalkylammonium salts, used as supporting electrolytes, were obtained from Southwestern Analytical Chemicals, dried for 12 h at 70 °C, and dissolved without recrystallization in Aldrich Gold Label solvents.

Syntheses

The parent ligand methyl-2-amino-1-cyclopentenedithiocarboxylate was prepared by methods previously described with slight modifications [15a, 16]. *N*-Alkylamino derivatives of this material were synthesized by refluxing 1:1.1 ratios of the parent ligand and the appropriate *N*-alkylammine in methanol. A typical reaction involved dissolving 0.173 g of the parent ligand in 25 ml methanol and adding 1.2 ml of 70% aqueous methylammine solution. After refluxing for 3 h, a yellow precipitate formed, was extracted by vacuum filtration, washed with cold absolute ethanol, and dried in a vacuum dessicator. The free ligands decompose slowly from exposure to moisture. The compounds were recrystallized from either benzene or dioxane, yielding fine yellow plates of satisfactory elementary analysis.

Anal. Calc. for $C_8H_{13}NS_2$ (La): C, 51.28; H, 7.01; N, 7.48; S, 34.22. Found: C, 51.14; H, 6.98; N, 7.44; S, 34.60%.

Calc. for $C_9H_{15}NS_2$ (Lb): C, 53.68; H, 7.52; N, 6.92; S, 31.77. Found: C, 53.72; H, 7.55; N, 6.92; S, 31.77%.

Calc. for $C_{10}H_{17}NS_2$ (Lc)): C, 55.76; H, 7.97; N, 6.50; S, 29.69. Found: C, 55.80; H, 7.99; N, 6.50; S, 29.69%.

Calc. for $C_{11}H_{19}NS_2$(Ld): C, 57.58; H, 8.39; N, 6.11; S, 27.95. Found: C, 57.60; H, 8.39; N, 6.08; S, 27.88%.

The corresponding Zn(II), Ni(II) and Cu(II) complexes were synthesized by adding an alcoholic metal(II) acetate solution to a stirring solution of *N*-alkylammine also dissolved in alcohol. All syntheses except for the copper complexes required reflux times of 1–5 h. Copper syntheses were carried out at ice bath temperatures yielding precipitates within a matter of minutes. Reactions were typically performed on a millimolar scale in 20–50 ml of solvent. Colored precipitates formed and were collected by filtration, washed with cold absolute ethanol, and dried *in vacuo*. All compounds were stable with respect to dioxygen and moisture in the solid state. Nickel(II) complexes were recrystallized from dichloromethane/ethanol mixtures, while Cu(II) complexes exhibited instability in solution over extended time periods, decomposing into brown tars. All elemental analyses were satisfactory.

Anal. Calc. for $NiC_8H_{12}NS_2$ (**1a**): C, 44.55; H, 5.57; N, 6.49; S, 29.70. Found: C, 43.41; H, 5.65; N, 6.67; S, 28.81%.

Calc. for $NiC_9H_{14}NS_2$ (**1b**): C, 47.05; H, 6.16; N, 6.10; S, 27.91. Found: C, 46.99; H, 6.20; N, 6.09; S, 27.89%.

Calc. for $NiC_{10}H_{16}NS_2$ (**1c**): C, 49.28; H, 6.57; N, 5.75; S, 26.28. Found: C, 49.30; H, 6.69; N, 4.80; S, 26.25%.

Calc. for $NiC_{11}H_{18}NS_2$ (**1d**): C, 51.26; H, 6.99; N, 5.44; S, 24.85. Found: C, 51.06; H, 7.04; N, 5.43; S, 24.75%.

Calc. for $CuC_8H_{12}NS_2$ (**2a**): C, 44.09; H, 5.51; N, 6.43. Found: C, 43.67; H, 5.47; N, 6.38%.

Calc. for $CuC_9H_{14}NS_2$ (**2b**): C, 46.60; H, 6.04; N, 6.04. Found: C, 46.05; H, 6.02; N, 5.99%.

Physical measurements

Electronic absorption spectra of dichloromethane solutions and nujol mulls were recorded on a Cary 2300 spectrophotometer over the UV–Vis and near-IR region. The data were collected and manipulated with an Apple IIe computer.

All elemental analyses were obtained from Atlantic Microlabs, Atlanta, GA, U.S.A., and were satisfactory.

Electrochemical properties were determined in solutions of dichloromethane and dimethylformamide, with tetraalkylammonium perchlorate salts as supporting electrolytes, and using conventional three compartment H cells. A BAS CV 27 potentiostat and YEW model 3022 A4 X-Y recorder were used in all cyclic voltammetry experiments. Measurements were made using a platinum disk working electrode and platinum wire auxiliary electrode, with potentials standardized with the ferrocene/ferrocenium couple ($E_{1/2} = +0.37$ V in acetonitrile) against a saturated calomel electrode.

Solution ^1H NMR spectra were obtained on either a GE 300 MHz Omega FT-NMR, a GE 500 MHz Omega FT-NMR, or an IBM NR 100AF NMR spectrometer, the latter two both being equipped with variable temperature apparatus. All ^1H spectra were obtained using $CDCl_3$ solutions with TMS as an internal standard.

Electron spin resonance spectra were obtained at 120 and 300 K with a Varian E-3 spectrometer operating near 9 MHz (X band). Frozen glass spectra were obtained using 50/50 (by volume) dimethylformamide (DMF)/dichloromethane (CH_2Cl_2) solutions. Room temperature spectra were obtained as toluene solutions. Magnetic fields were calibrated with $VO(acac)_2$, and g values were standardized against the absorption of diphenylpicrylhydrazine (DPPH) at $g = 2.0036$.

Results

Electronic absorption

Absorption spectra for the series were obtained in the UV–Vis and near-IR regions over the range from 40 000 to 5000 cm^{-1}. The results appear in Tables 1 and 2 for solution and solid samples, respectively, of both the nickel and copper complexes. The nickel derivatives (**1**) exhibit broad, weak transitions in the range from 14 000–18 000 cm^{-1} typical for square planar d^8 complexes [17]. A common charge transfer appears in each spectrum of the

TABLE 1. Electronic spectral data of Ni(II) (**1**) and Cu(II) (**2**) complexes in dichloromethane

Compound	λ_{max} (kK) (ϵ (cm^{-1} mol^{-1}))
1a	34.48(10150), 30.30sh, 25.64(5000), 22.22(2950), 15.04(300)
1b	34.48(11350), 24.57(9750), 22.47sh, 21.64(7000), 14.71(500)
1c	34.48(10450), 29.41sh, 25.32(3500), 21.74(1250), 15.15(350)
1d	34.48(10000), 25.64(3200), 22.22(1000), 15.15(400)
2a	34.48(11200), 29.41(9700), 26.14(6000), 24.84sh, 16.74(1000), 12.08(25)
2b	36.36(11300), 29.03(9000), 25.91(6000), 16.33(1000), 11.85(30)

TABLE 2. Electronic spectral data for Ni(II) (1) and Cu(II) (2) complexes in the solid state as nujol mulls

Compound	λ_{max} (kK) (ϵ (path length^{-1} conc.$^{-1}$))[a]
1a	31.54(20070), 25.06(19600), 21.76(17800), 20.12sh, 15.00(12200)
1b	31.44(21770), 25.31(24512), 20.83(18300), 14.73(16150)
1c	31.86(24400), 25.45(24000), 21.01(16570), 15.10(14400)
1d	31.84(20700), 25.25(19460), 21.32(16200), 15.15(10100)
2a	34.84(19100), 29.15(14900), 25.91(14300), 24.15(14200), 20.62(12700), 16.67(11900), 11.90(11000), 8.47(8800)
2b	34.48(24250), 29.33(21500), 25.91(20550, 20000), 21.37(18400), 16.41(17700), 11.76(18400), 8.37(14400)

[a]All extinction coefficients are relative rather than absolute.

TABLE 3. Electrochemical data on Ni(II) (1) and Cu(II) (2) species. All values in mV vs. SCE[a]

Complex	$E_{ox}2$	$E_{ox}1$	$E_{1/2,red}(\Delta E_p)$
1a[b]	+725*i*	+575*i*	−1290(70)
1b	+725*i*	+625*i*	−1285(70)
1c		+680*i*	−1320(70)
1d		+690*i*	−1320(70)
2a[c]	+700*i*	+380*i*	−520(70)
2b	+730*i*	+510*i*	−470(69)

[a]All solutions 1 mM with 0.1M TEAP as supporting electrolyte. [b]Solvent CH_2Cl_2. [c]Solvent CH_2Cl_2/DMF. *i* = irreversible.

Ni(II) complexes between 21 000–23 000 cm^{-1} and is assigned as a S–M(II) LMCT. Strong MLCT, π–π^* and n–π^* transitions occur at higher energies.

Solid state absorption spectral data on the copper complexes were obtained on diffuse mulls and are typical of d^9 systems [3]. Low energy d–d transitions are well resolved for **2a** and **2b**, but are reported with relative extinction coefficients due to the unknown pathlength and concentration of the individual mulls. The red shift in ligand field transition energies represents a distortion towards a more tetrahedral geometry. The band in the 16.5 kK region could be attributed to either a strong d–d transition, which is uncharacteristic of pseudo-square planar Cu(II) complexes, or a weak S–Cu(II) LMCT. Given the ligand structures, the expected structure of the complexes, and the magnitude of the molar extinction coefficients, the low energy absorption is tentatively assigned as charge transfer. A higher energy MLCT blue shifts from a shoulder at 24.8 kK for **2a** to a shoulder embedded under the 25.9 kK absorption of **2b**. Decomposition of the Cu(II) complexes **2a** and **2b** in solution can be traced by noting the intensity of the peak in the 16 kK region diminish.

Electrochemistry

All the complexes were characterized electrochemically by cyclic voltammetry (CV) in both coordinating and non-coordinating solvents (DMF and CH_2Cl_2). $E_{1/2}$ values are reported in Table 3, where all values are referenced to a saturated calomel electrode. Scan limits were confined by the solvent window to +1.75 to −1.20 V for CH_2Cl_2 and +1.90 to −2.00 V for DMF. Irreversible oxidations are attributed to decomposition of the Ni(III) and Cu(III) products. A second anodic process indicates the oxidation of the thiolate ligands. Two separate oxidations are observable in the cases of Ni(II) **1a** and **1b**. The first of the two appear at +0.575 and +0.625 V for **1a** and **1b**, respectively, and are characteristic of metal centered oxidations which, judging from the lack of a corresponding reduction process, lead to decomposition of the complex in both cases. The second peak occurs at +0.720 V for both **1a** and **1b** and appears to be a destructive, ligand based oxidation process with a coupled reduction lying 200 mV negative and severly broadened. The oxidation couple for Ni(II) **1c** and **1d** shows a broad two electron process indicating merger of the two potentials for the metal and ligand centered processes. All reductions appear quasi-reversible, with $i_{p,a}/i_{p,c}$ ratios approaching unity and current passages exhibiting one electron processes. Half-wave reduction potentials also show some disparity between **1a** and **1b**, and **1c** and **1d**. **1b** exhibits a reduction potential of −1.280 V, slightly lower than that for **1a**, at −1.290 V. Reduction of **1c** and **1d** occur at virtually the same half-wave potentials, −1.320 V. Solvent dependence is minimal, indicating strictly four coordinate structures exist in solution.

Cyclic voltammograms on the resultant blue–green solutions of the copper complexes showed features similar to those of the nickel derivatives: distorted oxidation and quasi-reversible reduction processes. There are only small differences between the spectra of the two Cu(II) complexes. Oxidation potentials appear at about +0.500 and +0.720 V as reported in Table 3, and are assigned as metal based and ligand based processes, respectively. Both are electrochemically and chemically irreversible, resulting in decomposition of the starting material. Cu(III) complexes typically prefer planar stereochemistries which, due to steric hindrance in the present ligands, cannot be stabilized. One reversible reduction attributed to a Cu(II)/Cu(I) couple occurs at about +0.5 V for each complex. Integration of the area

beneath both cathodic and anodic peaks leads to an $i_{p,a}/i_{p,c}$ ratio of 1. Peak to peak potentials of about 70 mV are typical of reversible behavior in non-aqueous solvents.

Electron spin resonance

ESR data were obtained on the blue–green solutions of all four copper complexes, and are reported in Table 4. For comparison, the values obtained for the Cu(II) complexes of the bridged, tetradentate ligand systems are also listed. Figure 2 displays an X-band frozen glass spectrum for Cu(II) **2b**, where $g_{\parallel} = 2.156$ and $A_{\parallel,Cu} = 137 \times 10^{-4}$ cm^{-1}. Solution and frozen glass spectra exhibit five line nitrogen superhyperfine splitting on the four line hyperfine splitting from Cu(II), $I = 3/2$. Frozen glass spectra indicate inequivalence between g_{yy} and g_{xx}.

Nuclear magnetic resonance

Room temperature ^{1}H NMR spectral data are provided in Table 5. Figure 3 gives a representation of the structure of the complexes, showing the atomic labelling scheme used. Spectra of the Ni(II) (**1**) complexes varied significantly from spectra of the free ligands and diamagnetic Zn(II) (**3**) complexes. Despite obvious paramagnetic influence, all resonances remain detectable, with only the N-CH_2 (C8) protons showing line broadening. Integrated intensities, coupling and comparisons with spectra of similar complexes aided in the assignment of resonances. The protons of the first carbon in the R-group consistently exhibit the farthest downfield shift due to their proximity to the coordinating nitrogen. The effect rapidly attenuates over the neighboring protons in the longer R-groups, resulting in progressively smaller shifts from the respective free ligand, or diamagnetic zinc complexes resonances. The protons of the cyclopentene moiety experience the effects of the odd spin through communication with the π-system of the chelate ring. Protons on carbon 5 are shifted upfield; carbon 7, downfield. The S-CH_3 protons and those of C6 shift only slightly in each case. In order to verify the isotropic nature of the shifts, all samples were analyzed by NMR between 20 and 60° in deuterated chloroform solutions. All shifts were exaggerated at greater temperatures, without loss of resolution. Table 6 lists the shifts in resonances for **1d** at various temperatures. The data are representative of the isotropic behavior of the resonances of each Ni(II) complex.

Discussion

Previous success in the synthesis and characterization of M(II)N_2S_2 complexes of **4** and **5** led us to the present work with bis-bidentate complexes **1**, **2** and **3**. By 'breaking' the bridge between the two 'halves' of the tetradentate ligands we sought to stabilize N_2S_2 complexes with even greater tetahedral distortion. Introducing straight alkyl chains of increasing length offered a stepwise steric driving force to produce neutral molecules coordinating with intermediate stereochemistries in the square planar–tetrahedral equilibrium. The results conclusively present evidence for small changes in inner coordination geometries for both nickel and copper complexes.

Ni(II) complexes

Detailed analysis of solution and solid state electronic transitions reveal subtle red shifts in the highest d–d transition which are common for series of molecules with similar ligands, but varying coordination geometries. The values for the Ni(II) **1** series ligand field transitions are slightly higher in energy than those for the **4** series as a result of coordination in the *trans* configuration. The absorptions in the 22 kK region of the Ni(II) complexes are thought to involve a pπ–dπ S–Ni(II) transition. The energy and intensity of these LMCT bands provide a measure of S–Ni(II) bond covalency and subsequent delocalization of charge throughout the chelate ring of each ligand. Interestingly, **1b** exhibits the lowest LF and LMCT transition energies, suggesting greatest

TABLE 4. Electron spin resonance values for Cu(II) species (**2**), and of the bridged, tetradentate ligands (**5**) where $n = 2$, 3 and 4[a]

Species	g_i[b]	$A_{i,Cu}$[b]	$A_{i,N}$[c]	$g_{\parallel}$[c]	$A_{\parallel}$[c]
2a	2.078	60.1	11.2	2.140	142
2b	2.084	59.5	10.5	2.156	137
5 $n=2$[d]	2.055	81.1	13.2	2.117	181
5 $n=3$[d]	2.060	65.3	12.0	2.132	160
5 $n=4$[d]	2.066	55.9	9.1	2.140	145

[a]ESR hyperfine splittings ± 0.5 10^{-4} cm^{-1}. g values ± 0.002. [b]Obtained in toluene at ambient temperature. [c]Obtained in 50/50 DMF/CH_2Cl_2 as frozen glass, 100 K. [d]Values taken from ref. 4c.

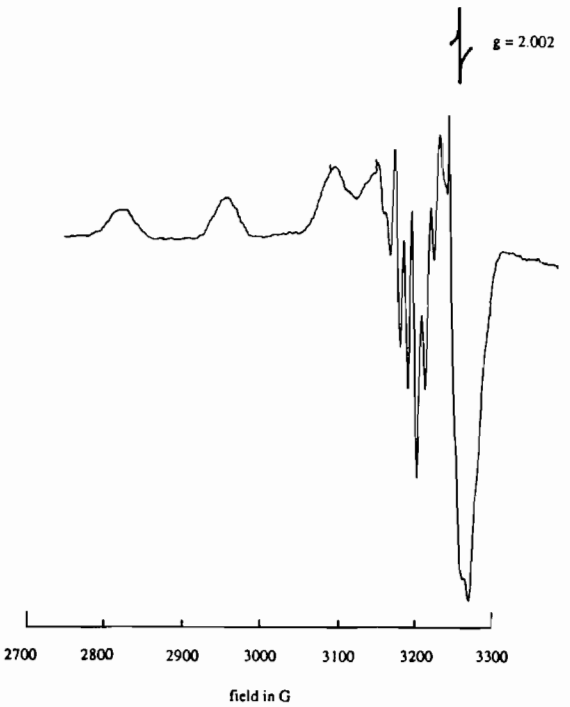

Fig. 2. ESR spectrum of Cu(II) R = et (**2b**) in 50/50 DMF/CH_2Cl_2 frozen glass at −100 K. Microwave frequency 9.117 GHz (X band).

coordination geometry distortion and S–M(II) covalency exists at this point in the series. The reversible Ni(II)/Ni(I) reductions also support the assignment of a more distorted, pseudo-tetrahedral geometry for the Ni(II) complex with R = ethyl.

More evidence supporting maximum distortion for **1b** resulted from ^1H NMR studies of the Ni(II) complexes. Initially, NMR spectral data were used to establish purity of the samples and confirm loss of the N–H resonance appearing near 12.5 ppm in the free ligands. Room temperature spectra revealed significant paramagnetic contributions from Ni(II), shifting resonances as far as 105 ppm downfield and −21 ppm upfield with respect to TMS. Shifting from square planar to tetrahedral stereochemistries results in spin state transition between diamagnetic and paramagnetic ground states. The magnitude of this mixing increases as a function of temperature and degree of geometrical distortion. Four coordinate Ni(II) systems which participate in structural equilibria between square planar and tetrahedral stereochemistries have been studied extensively [17]. As in other similar complexes, the method of spin transfer involves spin polarization caused by ligand to metal antiparallel spin transfer, which delocalizes odd spin throughout the HOMO, effecting the shielding tensors of the ligand nuclei, including the outerlying protons. Spin transfer from ligand to metal occurs predominantly through the S–Ni(II) bonds. This bonding interaction is very sensitive to the inner coordination environment, producing subtle changes in the energy spacing and occupancy of the metal d orbitals as the stereochemistry distorts from square planar to tetrahedral symmetry. As a result of these geometrical changes, the bonding molecular orbital with predominate $d_{x^2-y^2}$ character drops in energy while the antibonding molecular orbital, mostly of d_{xy} character, raises. As the energy separation between the filled d_{xy} MO and unfilled $d_{x^2-y^2}$ MO reduces to a value close to that of the pairing energy required to maintain a low spin diamagnetic singlet ground state, the high spin paramagnetic configuration becomes thermally accessible. Ultimately, the two orbitals would become degenerate in pure T_d symmetry, and result in a paramagnetic ground state triplet. Thus, increasing the temperature acts to increase the proportion of paramagnetic character within the

TABLE 5. NMR of free ligands (Lig), Zn (**3**) complexes and Ni (**1**) complexes. All values are reported ±0.005 ppm vs. TMS as an internal standard

Complex	1-CH_3	7-CH_2	6-CH_2	5-CH_2	N-H	8-CH_2	9-CH_2	10-CH_2	11-CH_2
Lig **a**	2.597	2.834	1.891	2.703	12.250	3.088			
3a	2.595	2.749	1.810	2.637		3.149			
1a	2.441	19.150	1.774	−9.210		40.481			
Lig **b**	2.579	2.803	1.891	2.698	12.350	3.405	1.316		
3b	2.591	2.705	1.800	2.654		3.435	1.134		
1b	2.398	37.254	1.506	−20.549		104.035	4.518		
Lig **c**	2.578	2.803	1.866	2.695	12.350	3.334	1.718	1.024	
3c	2.590	2.815	1.888	2.698		3.410	1.638	1.034	
1c	2.521	13.377	1.726	−4.748		37.363	3.057	1.855	
Lig **d**	2.566	2.792	1.837	2.765	12.420	3.416	1.561	1.536	0.876
3d	2.583	2.804	1.849	2.770		3.422	1.620	1.428	0.902
1d	2.503	13.965	1.734	−5.181		35.971	3.039	2.331	1.328

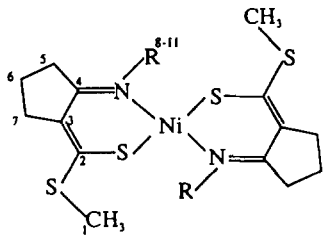

Fig. 3. Structure and labelling scheme used for NMR assignments in $M(II)N_2S_2$ complexes.

sample and increase spin polarization in the π-system of the ligand orbitals. Unequal contributions from opposing electron spins leave a pattern of excess odd spin on alternating nuclei in the six membered chelate ring [17c]. The pattern is depicted in Fig. 4 by the positions of the arrows. Excess odd spin on C4 causes the protons on the methylene C7 to shift upfield with respect to TMS. The opposite effect is experienced by the protons of C5, which shift downfield with increased paramagnetic influence.

Paramagnetic contact shifts are caused by electron–electron and nuclear–electron magnetic coupling between unpaired electrons on the metal and electrons from filled orbitals centered on the ligand [17a]. Planar chelates with delocalized π-systems are especially susceptible to ^1H resonance shifts caused by paramagnetic metal ions. Spin transfer mechanisms are separated into two different classifications: contact and dipolar. The nature of the observed shifts for **1a–d** indicate they arise from a Fermi contact mechanism which delocalizes odd spin through the ligand orbitals. Dipolar shifts arise from through space interactions and are normally considered negligible for systems similar to the present series of compounds. Since the shifts exhibit a linear relationship with temperature, the following relationship holds true [18c]:

$$\Delta f_o/f_i = -a_i(g_e/g_H)\{[g\beta S(S+1)]/6SkT\} \times [\exp(-\Delta G/RT)+1]^{-1} \quad (1)$$

In (1) Δf_o is the difference, or shift, in resonance for any given proton between analogous diamagnetic and paramagnetic molecules, f_i is the frequency of the NMR instrument, a_i is the electron-nuclear hyperfine coupling constant in Gauss, and g is the g value of the paramagnetic form. The remaining symbols have their usual meanings. The bracketed exponential term, $[\exp(-\Delta G/RT)+1]^{-1}$, represents N_p, the fraction of paramagnetic character of the sample in solution at temperature T, or the fractional proportion of twist in the inner coordination sphere from square planar to tetrahedral geometry. The zinc(II) derivatives were used as diamagnetic references.

Using the shift values for the protons of C5 and C7, and a_i values imported from a suitable tetrahedral, paramagnetic compound [17c], values for N_p were calculated and appear in Table 7. N_p calculated for a similar tetradentate Ni(II) complex, ***4*** $n=4$, was approximately 3% [14], a small value considering the dihedral angle between the NiNN′ and NiSS′ planes was 38°. The Ni(II) complex where the R-group is equal to ethyl exhibits the largest shifts of this series and, therefore, shows much more significant mixing of the low spin diamagnetic ground state with the high spin paramagnetic ground state. Such results agree well with the data obtained with electronic absorption measurements. The trend in N_p values suggests an appreciable difference in coordination geometries between **1a** and **1b**, and **1c** and **2d**. A possible explanation involves conversion from *cis* to *trans* binding configurations going from **1b** to **1c** caused by the increased steric repulsion of the alkyl substituents.

Sulfur coordination is regarded as a stabilizing force for low spin square planar geometries, however, rearrangement of the inner coordination sphere in favor of shorter Ni–S bond lengths provides additional stabilization [14a]. It appears in the present series that maximum Ni–S π overlap occurs with **1b**, suggesting the presence of an energy minimum in the square planar–tetrahedral equilibrium. Inclusion of Ni(II) in the delocalized π-system of the ligand also

TABLE 6. Variable temperature ^1H NMR of **1d**. Shifts (ppm) relative to TMS internal standard[a]

Temperature (°C)	C1	C5	C6	C7	C8	C9	C10	C11
22	2.55	−5.43	1.79	14.44	37.26	3.11	2.40	1.38
30	2.50	−6.85	1.75	16.22	42.38	3.19	2.50	1.43
40	2.51	−7.96	1.78	18.31	48.25	3.34	2.69	1.53
50	2.42	−9.41	1.72	20.35	54.16	3.38	2.763	1.54
58	2.40	−10.39	1.73	21.84	58.36	3.48	2.874	1.60

[a]Negative values indicate shifts upfield.

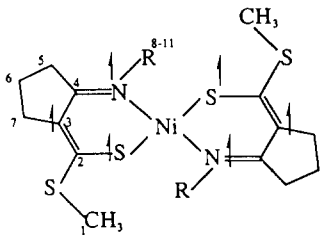

Fig. 4. Odd–alternate pattern of spin distribution over ligand framework.

TABLE 7. Contact shift analysis of Ni(II) complexes **1a–d**. Shift values for protons of carbons 5 and 7 were substituted into eqn. (1) in order to calculate N_p, or the fraction of paramagnetic molecules in the bulk sample at room temperature ($a_i = -0.683$ and -0.386, $g = 2$, $S = 1$)

Compound	$\Delta f_{i,iso}$C7 (ppm)	$\Delta f_{i,iso}$C5 (ppm)	$N_{p(av)}$ (%)	ΔG (kcal/mol)
1a	11.187	16.401	22.15	0.74
1b	34.549	17.937	42.43	0.18
1c	7.446	10.562	14.45	1.15
1c	8.223	11.669	15.28	1.01

creates stabilization for the divalent ion. As a result, oxidation potentials occur at negative values consistent with other non-physiological type ligand systems, values much lower than potentials seen in the native proteins (-390 to -640 mV versus SCE) [7].

Cu(II) complexes

The Cu(II) complexes are stable in the atmosphere, yet unstable in solution over time periods of 30 min to 1 h. Compounds **2a** and **2b** are isolated as dark green microcrystalline solids, and produce dark green–blue solutions upon dissolution in organic and inorganic solvents. The instability of Cu(II) in a tetrahedral coordination environment with respect to Cu(I) is well-documented, and indeed all indications are that these complexes decompose to yield a disulfide and Cu(I) species. Cu(I) prefers to coordinate in tetrahedral fashion, as is apparently the case for complexes with the n-propyl- and n-butyl-ligands. By taking advantage of the temporal stability of the Cu(II) species in solution, we were able to characterize **2a** and **2b** as d^9 systems. The reduction potentials for **2a** and **2b** are consistent with the trends observed for **5** $n = 2$, 3 and 4, and suggest significant distortion towards pseudo-tetrahedral stereochemistries. The values of -0.520 and -0.470 are intermediate between reduction potentials for other N_2S_2 complexes involving thiolate and thioether donor atoms [5]. The present ligand system coordinates through sulfur atoms which are strong σ- and π-donors, resulting in significant stabilization for Cu(II) ion, especially in a neutral environment. The distorted coordination geometry favors the reduced Cu(I) ion, however, yielding the slightly lower reduction potential of **2b** compared to **2a**. Continued efforts to stabilize CuN_2S_2 complexes with tetrahedral coordination environments should result in reduction potentials of even higher values.

Solution electronic absorption spectra are very similar in both complexes. The Cu(II) species absorb energy near 16 500 cm^{-1} with $\epsilon = 1000$ cm^{-1} M^{-1}, suggesting either an extremely intense d–d transition or a low energy charge transfer from sulfur to copper similar to the LMCTs in biological systems. At liquid nitrogen temperatures the absorption band appears more narrow, producing a sky blue colored solution.

The UV, visible and near-IR spectra of the complexes in the solid state as nujol mulls reveal very weak intensity ligand field bands at low energies for **2a** and **2b**, as well as the charge transfer bands in the 16 700 cm^{-1} region. Assuming C_2 symmetry and assigning a coordinate system with z as the primary axis and CuS_2 in the xz plane, four transitions between the d levels are permitted [14b]. Three transitions are expected to occur at similar energies: ^2B–$^2B_2$, ^2B–$^2A_1$ and ^2B–$^2A_2$, with the excited states $^2B_2$, $^2A_1$ and $^2A_2$ containing contributions from d_{x2-y2}, d_{xy} and d_{z2} orbitals. The fourth transition, $^2B_2$–$^2A_3$ occurs at lower energy, and involves the $^2A_3$ excited state, primarily d_{x2-y2} and d_{xy} in character. The first three transitions are expected at nearly similar energies, while the fourth occurs at a higher energy. **2a** and **2b** exhibit a broad absorption near 11.8 kK characteristic of a d–d transition. This value is close to the value reported for the Cu(II) center in Azurin, which has a band at 10.3 kK ascribed to a d–d transition. Calculations using a technique described by Companion and Komarynski [18] to determine ligand field transition energies revealed that manipulation of input variables biased in favor of larger tetrahedral distortion and weaker ligand fields effectively decreased the expected energies of the d–d bands.

The ESR spectra of the Cu(II) species were also interpreted. The reported g values (Table 4) indicate distortion from square planar geometry, yet are inconsistent with tetrahedral coordination. Rhombic g values with $g_{yy} \sim g_{xx} > 2.0$ indicate a d_{x2-y2} orbital ground state. An increase in $g_{\parallel}$ values and decrease in $A_{\parallel,Cu}$ values is expected upon transition from planar to tetrahedral environments. Small $A_{\parallel,N}$ values are indicative of weak nitrogen copper atomic overlap due to the mismatch in symmetry. Conversely, the soft sulfur donors are expected to benefit from

increased tetrahedral distortion causing the sulfur copper interaction to increase via increased $p\pi$–$d\pi$ S–M(II) bonding. The $A_{\parallel,Cu}$ value of 137×10^{-4} cm^{-1} determined for **2b** indicates significant tetrahedral distortion of the inner coordination sphere of a four coordinate Cu(II) species. A lower $A_{\parallel,Cu}$ value has been reported, but for a five coordinate complex [5c].

Comparisons to **5** $n=2$, 3 and 4 suggest inner coordination geometries in this series are slightly more distorted than 60°. Inclusion of Cu(II) in the delocalized chelating ring undoubtedly offers increased π-interaction favoring a low energy LMCT from the thiolate-like sulfur donors. Spectral properties also seem influenced by the degree of tetrahedral distortion, even to the point of stabilization of Cu(I) species. Fitting the ESR parameters onto an $A_{\parallel}$ versus $g_{\parallel}$ map provides a convenient method of comparison with other blue copper protein model systems, and indicates values for **2a–d** are lower than those of other synthetic molecules. The remarkably low values for the blue Cu(II) proteins, $A_{\parallel}=90-35\times10^{-4}$ cm^{-1}, could conceivably be attained with the present system if more tetrahedral geometries could be stabilized as Cu(II) species. We again stress the relationship between ESR parameters and twist angles of four coordinate N_2S_2 type complexes.

Conclusions

Neutral M(II)N_2S_2 complexes have been prepared and the relationship between spectral data and inner coordination sphere geometry have been investigated. Coordination geometries are influenced by steric repulsions caused by the addition of alkyl chains of varying length onto the coordinating nitrogens of the bidentate ligands. Reducing the symmetry of the inner coordination stereochemistry from D_{4h} to C_2, and pseudo-tetrahedral geometry, produces complexes with physical properties that indicate increased stability for both nickel(II) and copper(II) ions. Variable temperature NMR of the Ni(II) complexes revealed that the maximum tetrahedral distortion was achieved when the alkyl substituent was an ethyl group. Electrochemical oxidation potentials for the Ni(II) complexes are high compared to values found in nickel metalloenzymes, yet show a trend towards lower potentials accompanying more tetrahedral Ni(II)N_2S_2 coordination.

Cu(II)N_2S_2 complexes were also constructed with tetrahedrally distorted inner coordination spheres, resulting in a S–Cu(II) charge transfer band of similar energy to those in type I sites in proteins and ESR parameters that approach values in biological systems. Attempted preparations of complexes with increased distortion resulted in formation of Cu(I) species. An electronic absorption band occurs at 16 400 cm^{-1}, and hyperfine parameters reach $A_{\parallel,Cu}=137\times10^{-4}$ cm^{-1} and $A_{\parallel,N}=10.5\times10^{-4}$ cm^{-1} for **2b**. The resultant reduction potentials for the Cu(II)/Cu(I) couple are relatively low compared with the values of blue Cu(II) proteins, but exhibit a definite decrease as the coordination geometry twists towards tetrahedral symmetry. Although the present ligands do not accurately represent the type of donor atoms found at the site of the blue copper(II) proteins, spectral properties indicate the significant role that coordination geometry and S–Cu(II) interaction play in the optimization of the catalytic role of the native enzyme active site.

References

1 (a) T. G. Spiro (ed.), *Copper Proteins*, Wiley, New York, 1981, (b) K.D. Karlin and J. Zubieta (eds.), *Copper Coordination Chemistry: Biochemical and Inorganic Perspectives*, Vol. I, Adenine, New York, 1982.

2 W. E. Blumberg and J. Piesach, *J. Biochim. Biophys. Acta, 126* (1966) 269.

3 (a) H. J. Schugar, in K.D. Karlin and J. Zubieta (eds.), *Copper Proteins*, Wiley, New York, 1981; (b) K. D. Karlin and J. Zubieta (eds.), *Copper Coordination Chemistry: Biochemical and Inorganic Perspectives*, Vol. I, Adenine, New York, 1982.

4 (a) R. D. Bereman, J. R. Dorfman, J. Bordner, D. P. Rilemma, P. McCarthy and G. D. Shields, *J. Bioinorg. Chem.*, (1982) 49; (b) R. D. Bereman, M. W. Churchill and G. D. Shields, *Inorg. Chem., 18* (1979) 3117; (c) R. D. Bereman, G. D. Shields, J. Bordner and J. R. Dorfman, *Inorg. Chem., 20* (1981) 2165.

5 (a) L. Casella, M. Gullotti and R. Vigano, *Inorg. Chim. Acta, 124* (1986) 121; (b) L. Casella, M. Gullotti, A. Pintar, F. Pinciroli and R. Vigano, *J. Chem. Soc., Dalton Trans.*, (1989) 1161; (c) M. Gullotti, L. Casella, A. Pintar, E. Suardi, P. Zanello and S. Mangani, *J. Chem. Soc., Dalton Trans.*, (1989) 1979, and refs. therein.

6 (a) D. R. McMillin, *J. Chem. Educ., 62* (11) (1985) 997; (b) A. W. Addison, *Inorg. Chim. Acta, 162* (1989) 217.

7 (a) R. P. Hausinger, *Microbiol. Rev., 51* (1987) 22; (b) R. Cammack, *Adv. Inorg. Chem., 32* (1988) 297; (c) J. Lancaster (ed.), *The Bioinorganic Chemistry of Nickel*, VCH, New York, NY, 1988.

8 (a) D. V. DerVartanian, H.-J. Krüger, H. D. Peck, Jr. and J. LeGall, *Rev. Port. Quim., 27* (1975) 70; (b) S. P. J. Albracht, A. Kroger, J. W. Van der Zwaan, G. Unden, R. Bocher, H. Mell and R. D. Fontijn, *Biochim. Biophys. Acta, 874* (1986) 116; (c) P. A. Lindahl, N. Kojima, R. P. Hausinger, J. A. Fox, B. K. Teo, C. T. Walsh and W. H., Orme-Johnson, *J. Am. Chem. Soc., 106* (1984) 3062; (d) R. A. Scott, S. A. Wallin, M. Czechowski, D. V. DerVartanian, J. LeGall, H. D. Peck, Jr. and I. Moura, *J. Am. Chem. Soc., 106* (1984) 6864; (e) S. P. Cramer, M. K. Eidsness, W.-H. Pan,

T. A. Morton, S. W. Ragsdale, D. V. Der Vartanian, L. G. Ljungdahl and R. A. Scott, *Inorg. Chem., 26* (1987) 2477.

9 (a) H.-J. Krüger and R. H. Holm, *Inorg. Chem., 27* (1988) 3645; (b) W. R. Pangratz, F. L. Urbach, P. R. Blum and S. C. Cummings, *Inorg. Nucl. Chem. Lett., 9* (1973) 1141; (c) R. M. C. Wei and S. C. Cummings, *Inorg. Nucl. Chem. Lett., 9* (1973) 43; (d) P. R. Blum, R. M. C. Wei and S. C. Cummings, *Inorg. Chem., 13* (1974) 450. (e) L. S. Chen and S. C. Cummings, *Inorg. Chem., 17* (1978) 2358; (f) M. F. Corrigan and B. O. West, *Aust. J. Chem., 29* (1976) 1413. (g) I. Bertini, L. Sacconi and G. P. Speroni, *Inorg. Chem., 11* (1972) 1323. (h) K. Nag and D. S. Joardar, *Inorg. Chim. Acta, 14* (1975) 433. (i) S. K. Mondal, P. Paul, R. Roy and K. Nag, *Transition Met. Chem., 9* (1984) 247. (j) R. Roy, P. Paul and K. Nag, *Transition Met. Chem., 9* (1984) 152; (k) S. K. Mondal, D. S. Joardar and K. Nag, *Inorg. Chem., 17* (1978) 191.

10 M. G. Kanatzidis, *Inorg. Chim. Acta, 168* (1990) 101.

11 H. J. Krüger and R. H. Holm, *Inorg. Chem., 28* (1989) 1148.

12 (a) T. Yamamura, *Chem. Lett.,* (1986) 801; (b) T. Yamamura, H. Miyamae, Y. Katayama and Y. Sasaki, *Chem. Lett.,* (1985) 269; (c) D. G. Holah and D. Coucouvanis, *J. Am. Chem. Soc., 97* (1975) 6917; (d) D. Swenson, N. C. Baenziger and D. Coucouvanis, *J. Am. Chem. Soc., 100* (1978) 1933; (e) R. W. Lane; J. A. Ibers, R. B. Frankel, G. C. Papefthymiou and R. H. Holm, *J. Am. Chem. Soc., 99* (1977) 84; (f) S. G. Rosenfield, W. H. Armstrong and P. K. Marsharak, *Inorg. Chem., 25* (1986) 3014.

13 (a) R. Cammack, D. S. Patil, E. C. Hatchikian and V. M. Fernande, *Biochim. Biophys. Acta, 98* (1987) 912; (b) D. L. Tennent and D. R. McMillin, *J. Am. Chem. Soc., 101* (1979) 2307; (c) V. Lum and H. B. Gray, *Isr. J. Chem., 21* (1981) 23; (d) H. R. Engeseth, D. R. McMillin and E. L. Ulrich, *Inorg. Chim. Acta, 67* (1982) 145; (e) J. A. Blaszak, E. L. Ulrich, J. L. Markley and D. R. McMillin, *Biochemistry, 21* (1982) 6253.

14 (a) E. M. Martin, R. D. Bereman and J. R. Dorfman, *Inorg. Chim. Acta, 176* (1990) 247; (b) E. M. Martin, R. D. Bereman and P. Singh, *Inorg. Chem., 30* (1991) 957.

15 (a) T. Takeshima, M. Yokoyama, Tsusneo, T. Imamoto, A. Makiko and H. Asaba, *J. Org. Chem., 34* (1969) 730; (b) P. Bordas, P. Sohar, G. Matolcsy and P. Berencsi, *J. Org. Chem., 37* (1972) 1727.

16 R. S. Drago, *Physical Methods in Chemistry,* Saunders, Philadelphia, PA, 1977, pp. 387–391.

17 (a) R. H. Holm, G. N. in La Mar, W. D. Horrocks and R. H. Holm (eds.), *NMR of Paramagnetic Ions,* Academic Press, New York, 1973, pp. 243–326; (b) R. H. Holm, *Acc, Chem. Res., 2* (1969) 307; (c) D. H. Gerlach and R. H. Holm, *J. Am. Chem. Soc., 91* (1969) 3457; (d) G. W. Everett, R. H. Holm and A. Chakravorty, *Prog. Inorg. Chem., 7* (1966) 83; (e) G. W. Everett and R. H. Holm, *Inorg. Chem., 7* (1968) 776; (f) *J. Am. Chem. Soc., 87* (1964) 2117.

18 A. L. Companion and M. A. Komarynski, *J. Chem. Educ., 41* (1964) 257.